Polish Society of Composite Materials
Polskie Towarzystwo Materiałów Kompozytowych

23: 2 (2023) 89-96

COMPOSITES THEORY AND PRACTICE
ISSN: 2084-6096
ISSN (online): 2299-128X

**D.V. Praveen[1, 2]*, M.V.J. Raju[2], D.R. Raju[3]**

*[1]Department of Mechanical Engineering, Bapatla Engineering College, Bapatla, India*
*[2]Department of Mechanical Engineering, A.U.College of Engineering (A), Vishakhapatnam, India*
*[3]Formerly Principal, SRKR Engineering College, Bhimavaram, India*
** Corresponding author: E-mail: d.vijay.praveen@gmail.com*

*Received (Otrzymano) 22.01.2022*

# WEDM PARAMETRIC STUDY OF AA7075/6 wt.% Ni-COATED $Al_2O_{3(P)}$ COMPOSITE MINIATURE GEARS

**Nowadays, gears are essential components in various electro-mechanical devices. Nevertheless, the fabrication of miniature-sized gears is very complicated. The present paper is focused on assessing the influence of the WEDM parameters on the material removal rate (MRR) and surface roughness (*Ra*) of AA7075/6 wt.% nickel-coated $Al_2O_3$ composite miniature gears. Initially, the theoretical design calculations were performed, and consequently the results were validated using ANSYS 19.0 software. Furthermore, experiments were modelled in accordance with Taguchi's $L_9$ orthogonal array. Optimal combinations of pulse on time, pulse off time and peak current were assessed using grey relational analysis (GRA) coupled with principal component analysis (PCA). The significance of the parametric influence on the machining responses was also evaluated using the ANOVA technique. Consequently, confirmation tests were conducted to verify the optimal parameters and the predicted results are in good agreement with the experimental findings.**

**Keywords:** wire-EDM, non-conventional machining, MRR, Ra, GRA-PCA

## INTRODUCTION

Rapid developments in the manufacturing sector cause an increase in the interest in composite materials with superior mechanical properties [1]. Currently, aluminium based metal matrix composites are being focused on due to their excellent properties, like good mechanical and tribological properties to fabricate complex shaped parts [2]. Among all power transmission elements, gears are employed in wide range of applications [3]. Miniature gears constitute the key mechanical elements used in robots, high-precision instruments, micro pumps, timer mechanisms, domestic appliances and medical equipment. The performance of a gear during its service time depends on the manufacturing quality [4]. Conventional miniature gear manufacturing methods are die casting, the powder metallurgy route, gear hobbing, stamping and extrusion processes, which do not meet the quality requirements of miniature gears [5]. To overcome the limitations effected by the conventional fabrication processes of miniaturized gears, wire-electrical discharge machining (WEDM) is extensively recognized for manufacturing such components owing to its excellent capabilities like the fabrication of burr-free products, in addition to high-quality surface integrity with good dimensional accuracy [6, 7].

Chaubey and Jain conducted investigations on the fabrication of miniature gears using the WEDM prototyping of miniature bevel gears and helical gears. Response surface methodology was adopted to design the experimental sets to measure the volumetric gear-cutting rate during wire-spark erosion machining. Interactions between the characteristics and the significance of the responses were studied using ANOVA. Furthermore, the tooth profile and surface texture were examined using SEM micrographs. From their experimental studies, it was observed that the pulse on time, servo voltage, pulse off time and wire feed were found to be significant parameters for both miniature bevel gears as well as helical gears [7]. Alhadeff et al. investigated the fabrication of brass miniature gears to increase the productivity of the fabrication of miniature gears using WEDM by maintaining good surface integrity with a good material removal rate. From their investigations, it was revealed that minimizing the recast layer by a second pass leads to an improved rate of production [8]. Chaubey and Jain described the influence of the process parameters on the tooth profile and surface quality of stainless steel meso bevel as well as helical gears during WEDM. From their experimental studies, it was observed that the best surface quality of the gears was achieved at lower pulse on time, higher pulse off time, lower current, peak current and a higher level of flushing pressure, wire feed rate and wire tension. It was also concluded that the WEDM process is the best alternative method to manufacture net-shaped gears with good quality [9]. Ali et al. conducted a comparison study on the machining of miniature spur gears on both conventional and micro WEDM. From their investigations, it was observed that for micro engineering applications, conventional WEDM can be utilized and the dimensional accuracy and surface quality are acceptable [10].

From the above literature review, it was noticed that WEDM studies on advanced materials like surface-treated ceramic particle reinforced composites, which possess superior properties compared to other composite materials, have not been conducted for the fabrication of miniature-sized gears. Therefore, the main objective of the present study is to investigate the capability of WEDM to manufacture the gears and also to explore the effect of the process parameters on the machining responses of AA7075/6 wt.% nickel-coated $Al_2O_3$ composites.

## MATERIALS AND METHODOLOGY

### Fabrication of composites

AA7075 was selected for the base material because of its superior characteristics like good wear resistance, better fatigue strength, average machinability and considerable corrosion resistance. The AA7075 rods were procured from M/s Vision Castings and Alloys, Hyderabad. $Al_2O_3$ microparticles were chosen as the reinforcement owing to their good properties like high hardness, good wettability and chemical stability. These particles, 2-20 micrometre (avg.) in size, 99% purity, were procured from M/s Aarshadhaatu Green Nanotechnologies India Private Limited, Guntur. The chemical content of the 7075 alloy in weight percentage is Zn 5.6%, Mg 2.3%, Cu 1.5%, Si 0.5%, Mn 0.5%, Ti 0.5%, Cr 0.5% and Al the rest. The electroless coating route was utilised to coat the $Al_2O_3$ particles according to ASTM B-733, as this coating technique possesses many benefits like uniform coating, a high production rate and simple process when compared with the other coating methods [11-14]. Nickel was selected as the coating material and the steps followed are presented in Figure 1.

After completion of the nickel coating process, a change in the colour of the particles was observed, which was a preliminary indication of the nickel deposition on the particles. Furthermore, morphological studies of the reinforcement were carried out by SEM (FEI-Quanta FEG200, USA) along with EDAX of the particles before coating and after coating. Stir casting methodology was chosen to produce the composite as it offers many promising benefits like simplicity and cost-effectiveness [15-16].

The content of 6 wt.% coated $Al_2O_3$ reinforcement was chosen for the present study. Initially the Ni-coated $Al_2O_3$ reinforcement was measured using a digital analytical balance and then they were preheated before being introduced into the hot melt. The stirring process was performed for 8 minutes at the speed of 350 rpm. Consequently, the fabrication of the composites was carried out by pouring the molten metal into a graphite mould and allowing it to solidify at room temperature.

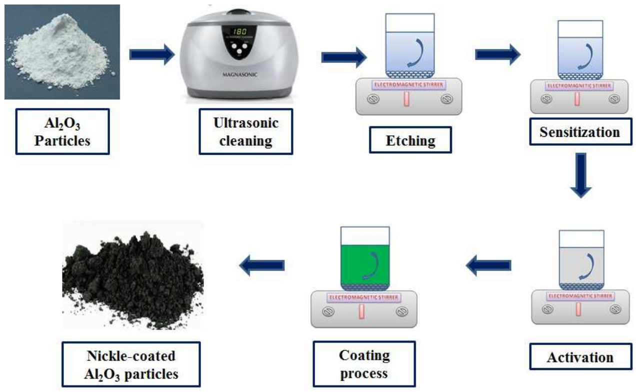


Fig. 1. Steps in $Al_2O_3$ particle coating [12]

### Design of spur gear

In power transmission gears, the power is transmitted by a force exerted by the driving gear tooth on the driven tooth gear. According to the law of gearing, normal force $F_n$ must always act along the line of action, which is tangent to the base circles of both gears. $F_n$ is inclined at the pressure angle with a centre line to both the gears at their pitch circles. Consequently, $F_n$ can be resolved in two components such as a tangential component ($F_t$) as well as radial component $F_r$. In the present work, a miniature gear is to be designed that can be used for 3D printers, robotic and medical equipment applications. The design parameters adopted for the fabrication of the miniature spur gears are shown in Table 1.

TABLE 1. **Design parameters of miniature gears**

| Terms | Symbol | Value |
|---|---|---|
| Module [mm] | $h_a$ | 0.9 |
| Pressure angle | $\alpha$ | $20^{\circ}$ |
| No. of teeth | $Z$ | 16 |
| Addendum [mm] | $h_a$ | 0.9 |
| Dedendum [mm] | $h_f$ | 1.125 |
| Tooth depth [mm] | $h$ | 1.575 |
| Bore diameter [mm] | $d$ | 6.00 |
| Fillet radius [mm] | $R$ | 0.36 |

The theoretical calculations of the bending stress and deflection are as below:

- Torque ($T$) = 411.8 N-mm ≈ 412 N-mm at 450 rpm

$$\text{Tangential load } (F_t) = 2T/d,$$

where $T$ is the torque, $d$ pitch circle diameter

$$F_t = (2\times412) / (14.1) = 58.4 \text{ N}$$

- Calculation for bending stress:

  Theoretical bending stress ($\sigma b$) = $F_t$ / (mbY)

  where $b$ is the face width and $Y$ the Lewis form factor (0.255 for 14.5° full depth)

  $$\sigma b = 58.4 / (0.9\times10\times0.255) = 25.44 \text{ N/mm}^2$$

- Calculation of deflection:

$$\delta l = Wl^3 / 3EI$$

$$l = h/2, \quad I = b \times t^3 / 12, \quad E = 83\ 000 \text{ N/mm}^2$$

$$h = \text{addendum} + \text{dedendum} = 0.9 + 1.125 = 2.025 \text{ mm}$$

$$= [58.4\times (1.0125\text{^}3)] / [3\times83\times10\text{^}3\times (10\times0.9\text{^}3)/12] = 0.000407 \text{ mm}$$

## Finite element analysis of composite miniature spur gear

Validation of the theoretical results of the AA-7075/6 wt.% nickel-coated $Al_2O_3$ composite miniature gear was performed utilising ANSYS 19.0 software. A solid model of a miniature gear was modelled and analysed using the workbench platform. The boundary conditions for the current model were assumed as the inner surface of the bore of the spur gear, which was fixed and exposed to surface load at the curved face of the gear tooth. A tangential force of 58.4 N was applied to the tip of the tooth of the spur gear by fixing the shaft diameter. The equivalent stresses occurring on the spur gear when the tangential force was applied were found to be 28.44 N/mm$^2$ and the total deformation of the observed maximum total deformation is 0.000497 mm. Views of the solid model and finite element model with boundary conditions, total deformation and equivalent stresses are shown in Figure 2.

## Machining parameters and responses

Based on previous machining studies conducted on the composites, it was observed that the pulse on time ($T_{on}$), pulse off ($T_{off}$) and peak current ($I$) exhibit a significant influence on the machining responses of the developed composites [17]. Thus, for the current analysis, the pulse on time, peak current and gap voltage were considered as the machining parameters. All the other parameters such as pulse off time, wire feed, wire tension and the flushing pressure of dielectric fluid were considered as fixed parameters. From the literature studies, it was noticed that the machining responses, such as the material removal rate (MRR) and surface roughness ($R_a$), are always given top priority in machining responses, as the quality of the machining is significantly influenced by MRR and $R_a$ [6, 18, 19]. MRR can be calculated using equation (1)

$$\text{MRR} = \text{mean speed} \times \text{thickness of material} \times \text{width of cut} \quad (1)$$

The surface roughness ($R_a$) of the machined surface was measured using a Surftest SJ-210 (Mitutoyo). An average of three readings were taken to determine the surface roughness of the machined samples.

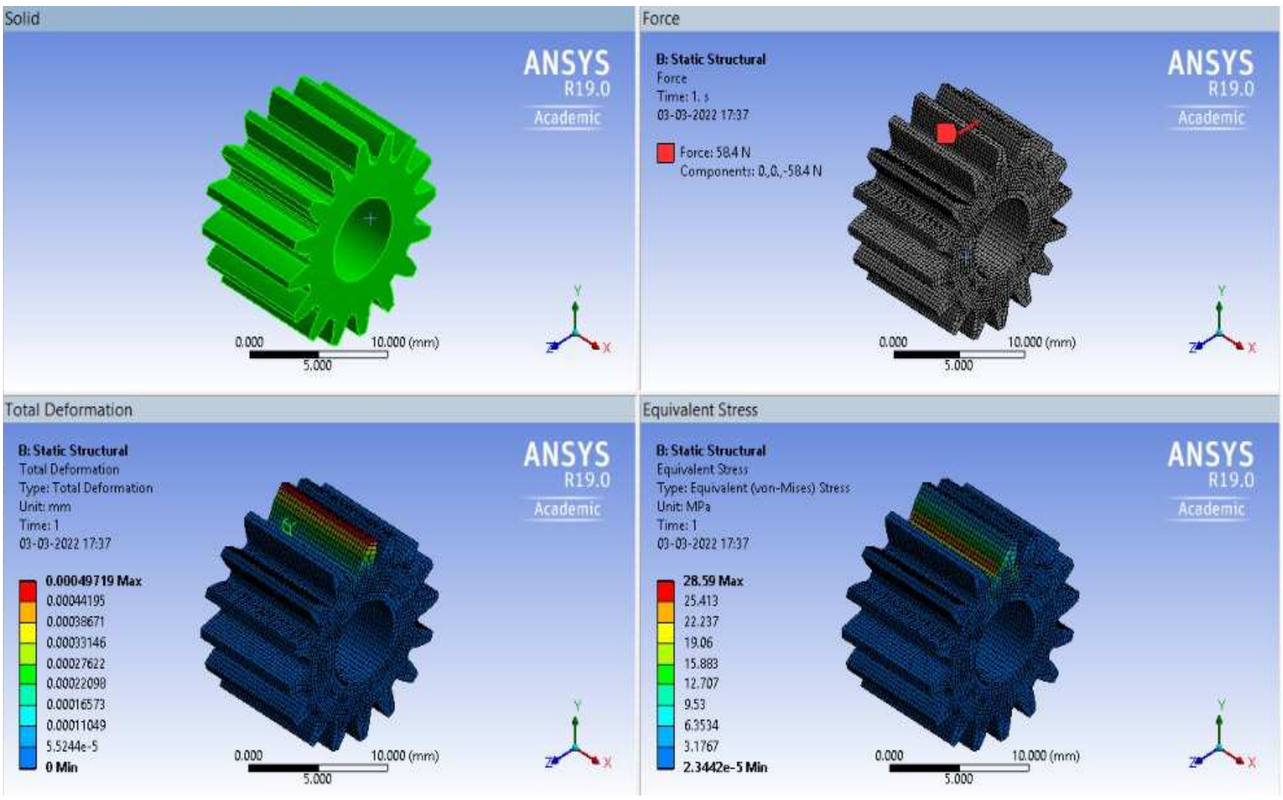

Fig. 2. Solid model and FE model of composite miniature gear

 

### Design of experiments (DoE)

The experiments were designed according to Taguchi's $L_9$ orthogonal array, using Minitab 19 software by considering 3 factors and 3 levels. The parameters with their levels are presented in Table 2.

TABLE 2. **Factors and levels**

| Factors | Notation | Levels | | |
|---|---|---|---|---|
| Pulse on [μs] | A | 122 | 124 | 126 |
| Pulse off [μs] | B | 45 | 50 | 55 |
| Peak current (A) | C | 155 | 160 | 165 |

### Analysis of responses using Taguchi's S/N Ratio

The machining responses, i.e. MRR and Ra, were evaluated using Taguchi's signal-to-noise (S/N) ratio. Based on the sort of quality elements, the S/N ratios of the responses were calculated, namely nominal the better, smaller the better and larger the better [20, 21]. The material removal rate must be maximized; therefore, the larger the best was chosen and determined by using Equation (2), and surface roughness with lower the best using Equation (3):

$$SN_{LB} = -10\log_{10}\left(\frac{1}{n}\sum_{i=1}^{n} 1/y_i^2\right) \quad (2)$$

$$SN_{SB} = -10\log_{10}\left(\frac{1}{n}\sum_{i=1}^{n} y_i^2\right) \quad (3)$$

### Optimization using grey relation analysis coupled with principal component analysis (GRA-PCA)

Grey relation analysis can be used to analyse the multi-objective problem by determining the machining responses into one single value to find feasible solutions [22]. This technique reduces the original problem into a single decision-making problem [23]. The methodology of the optimization studies is presented in Figure 3.

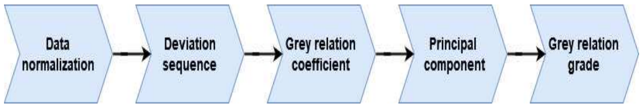


Fig. 3. Methodology in GRA coupled PCA

## RESULTS AND DISCUSSION

### Microstructural and basic mechanical properties

SEM micrographs of the particles are shown in Figure 4. In the micrographs, it can be seen that the uncoated particles have a very clean surface. The coated particles were observed to have rough surfaces with some elemental depositions. The presence of the nickel on the particles was confirmed by EDAX analysis.

SEM along with EDAX of composite with the 6 wt.% Ni-coated $Al_2O_3$ reinforcement is presented in Figure 5. The mechanical properties of the developed composites are listed in Table 3.

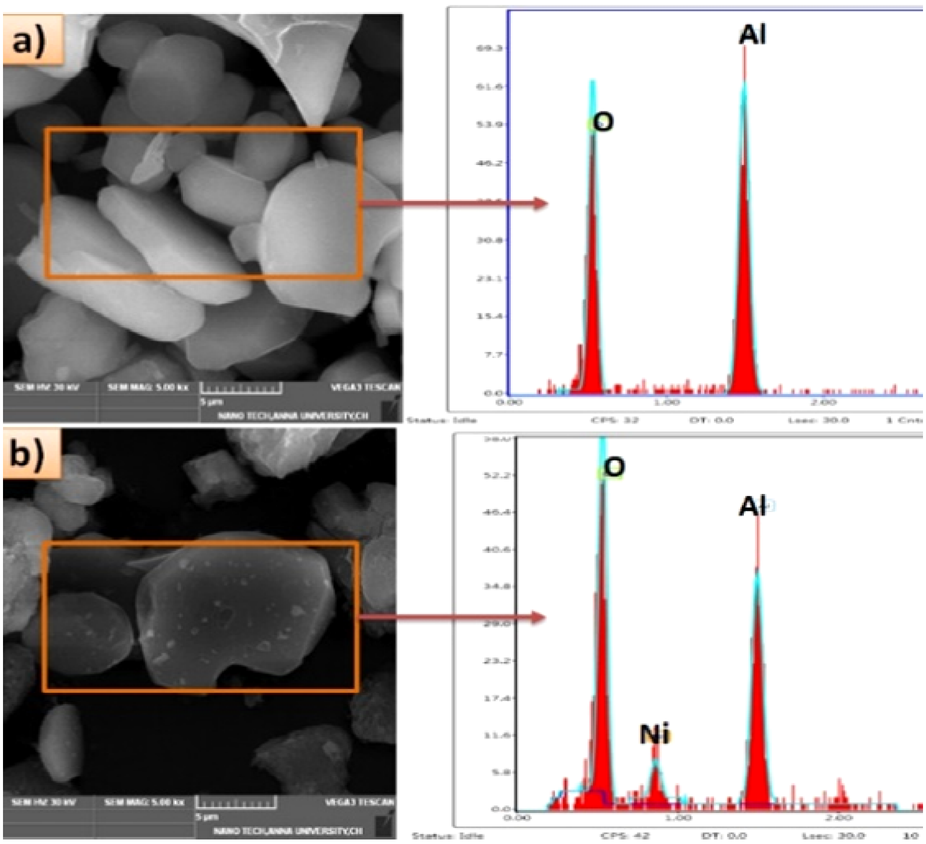


Fig. 4. SEM with EDAX of: a) pure and b) Ni-coated $Al_2O_3$ reinforcement

 

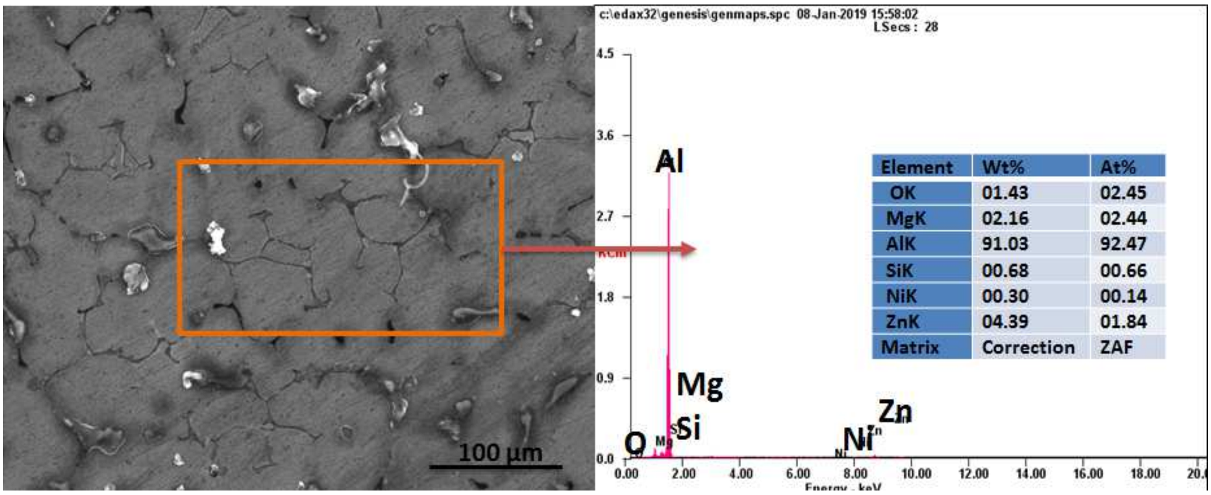


Fig. 5. SEM with EDAX of AA7075/6 wt.% Ni-coated $Al_2O_3$ composite

TABLE 3. **Basic mechanical properties of AA7075 6 wt.% $Al_2O_3$ composite [13]**

| S. No | Property | Value |
|---|---|---|
| 1 | Density | 2.790 gm/cm$^3$ |
| 2 | Hardness | 153 VH@ 200 gf |
| 3 | Tensile strength | 254 MPa |
| 4 | Young's modulus | 83 GPa |
| 5 | Poisson's ratio | 0.3 |

## Study of machining responses

6 wt.% nickel-coated alumina reinforced AA-7075 MMC plates with the dimensions 100 mm ×100 mm × × 10 mm were taken as the workpiece. The workpiece was machined into spur gears of 15 mm tip diameter by considering the machining parameters according to Taguchi's experimental design ($L_9$). The machined composite spur gears are shown in Figure 6 and the corresponding machining responses MRR and Ra are presented in Table 4.

Fig. 6. Fabricated miniature gears

TABLE 4. **WEDM experimental results**

| Exp. run | Machining factors | | | MRR [mm$^3$/min] | SR [µm] |
|---|---|---|---|---|---|
| | Pulse on [µs] | Pulse off [µs] | Peak current [A] | | |
| 1 | 122 50 | 45 130 | 155 | 2.663 | 2.989 |
| 2 | 122 50 | 50 130 | 160 | 2.698 | 2.867 |
| 3 | 122 50 | 55 130 | 165 | 2.676 | 2.701 |
| 4 | 124 54 | 45 130 | 160 | 2.859 | 3.248 |
| 5 | 124 54 | 50 130 | 165 | 2.861 | 3.117 |
| 6 | 124 54 | 55 130 | 155 | 2.738 | 3.258 |
| 7 | 126 58 | 45 130 | 165 | 3.035 | 3.387 |
| 8 | 126 58 | 50 130 | 155 | 2.914 | 3.539 |
| 9 | 126 58 | 55 130 | 160 | 2.918 | 3.407 |

## Influence of parameters on MRR

The main effects plot for the SN ratios of MRR is presented in Figure 7.

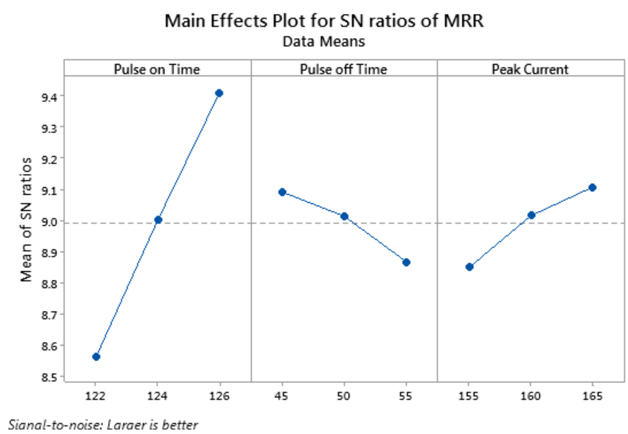


Fig. 7. Main effects plots of MRR

 

From the plots, it was observed that with the increase in the pulse on time, MRR was observed to increase due to the extended period of intensified sparks. MRR dwindled with the rise in the pulse off time as a consequence of the reduced spark discharge time. Furthermore, with the increase in the peak current, a superior metal removal rate was identified because of the increased and evenly distributed sparks at the cutting zone [24].

### Parametric influence of on $R_a$

The main effect plots for the S/N ratio of $R_a$ is shown in Figure 8. From the responses, it is seen that surface roughness was observed to grow with an increase in the pulse on time. This is a result of a rise in the produced thermal energy due to increased electrical sparks on the workpiece. Moreover, craters occur, which influenced the surface integrity of the gears. A better surface finish was observed with an increment in the pulse-off time. This is because of the increased pulse gap to flush out the additional volume of metal debris. What is more, this leads to a reduction in the re-solidification of molten material on the machined gear surface [25]. The surface roughness was observed to increase with the rise in the peak current because of well-distributed charge on the surface of the material. Owing to this, the produced craters are smaller in size. Consequently, better surface roughness was achieved [26].

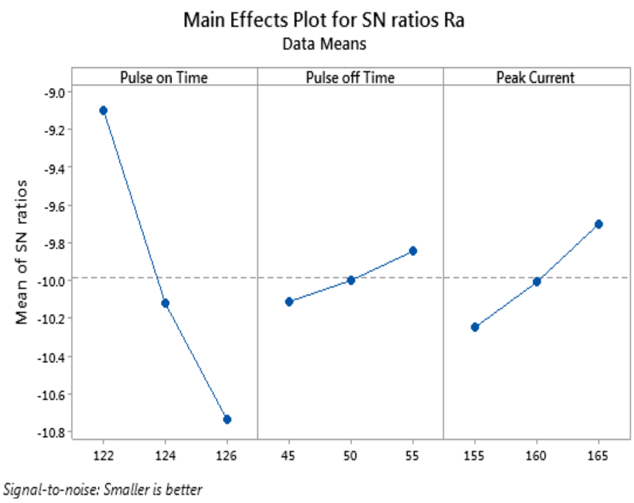


Fig. 8. Main effects plots of $R_a$

### Data analysis using Analysis of Variance (ANOVA)

The significance of the machining responses was determined by the ANOVA technique. The ANOVA of MRR and $R_a$ are presented in Tables 5 and 6. The tables show the parameters such as the degree of freedom (DoF), the sum of squares (SS), the mean of squares (MS), Fisher's ratio (F) and the probability value (P). From ANOVA, the most significant parameters for MRR and Ra were identified based on Fisher's value as the pulse on time, peak current and pulse off time.

TABLE 5. **ANOVA of MRR data**

| Source | DF | Seq SS | Adj SS | Adj MS | F value | P value |
|---|---|---|---|---|---|---|
| Pulse on | 2 | 0.1148 | 0.1148 | 0.0574 | 752.13 | 0.001 |
| Pulse off | 2 | 0.0086 | 0.0048 | 0.0043 | 56.45 | 0.017 |
| Peak current | 2 | 0.0112 | 0.1112 | 0.0056 | 73.55 | 0.013 |
| Error | 2 | 0.0001 | 0.0001 | 0.0000 | | |
| Total | 8 | 0.1348 | | | | |

TABLE 6. **ANOVA of $R_a$ data**

| Source | DF | Seq SS | Adj SS | Adj MS | F value | P value |
|---|---|---|---|---|---|---|
| Pulse on | 2 | 0.5327 | 0.5327 | 0.2663 | 3988.88 | 0.000 |
| Pulse off | 2 | 0.0112 | 0.0112 | 0.0056 | 84.37 | 0.012 |
| Peak current | 2 | 0.0564 | 0.0564 | 0.0282 | 422.42 | 0.002 |
| Error | 2 | 0.0001 | 0.0001 | 0.0000 | | |
| Total | 8 | 0.6004 | | | | |

### Multi-objective optimization using GRA-PCA

In the present study, GRA coupled with PCA was chosen to optimize the combined impact on the machining responses. The machining responses (i.e. MRR and $R_a$) have different units. As a result, these measurements were normalized according to GRA methodology. Then they proceeded to deviational sequence values to determine the grey relational coefficient. The GRA calculations are shown in Table 7.

TABLE 7. **GRA calculations**

| Exp. No. | Data normalization | | Deviational sequence | | Grey relation coefficient | | GRG | Rank |
|---|---|---|---|---|---|---|---|---|
| | MRR | $R_a$ | MRR | $R_a$ | MRR | $R_a$ | | |
| 1 | 0.000 | 0.656 | 1.000 | 0.344 | 0.333 | 0.593 | 0.463 | 8 |
| 2 | 0.094 | 0.802 | 0.906 | 0.198 | 0.356 | 0.716 | 0.536 | 3 |
| 3 | 0.035 | 1.000 | 0.965 | 0.000 | 0.341 | 1.000 | 0.671 | 2 |
| 4 | 0.527 | 0.347 | 0.473 | 0.653 | 0.514 | 0.434 | 0.474 | 6 |
| 5 | 0.532 | 0.504 | 0.468 | 0.496 | 0.517 | 0.502 | 0.509 | 4 |
| 6 | 0.202 | 0.335 | 0.798 | 0.665 | 0.385 | 0.429 | 0.407 | 9 |
| 7 | 1.000 | 0.181 | 0.000 | 0.819 | 1.000 | 0.379 | 0.690 | 1 |
| 8 | 0.675 | 0.000 | 0.325 | 1.000 | 0.606 | 0.333 | 0.470 | 7 |
| 9 | 0.685 | 0.158 | 0.315 | 0.842 | 0.614 | 0.372 | 0.493 | 5 |

From the GRA calculations, it was observed that experimental set 7 was found to a have higher grey relation grade. In this experimental set, (i.e. pulse on time 127 µs, pulse off time 45 µs and peak current at 165 A) a higher MRR and better $R_a$ were obtained due to intensified electric pulses with a sufficient time gap to flush out the metal pieces from the work material. The obtained responses were well correlated with the previous findings [24-26].

### Morphological studies of gears

After successful machining of the composite spur gears, morphological studies of the gear which was machined employing optimal parametric set 7, were carried out using SEM along with EDAX (Fig. 9) to check the surface irregularities. Surprisingly, the surface of the gear teeth was free from craters, burrs, globules, voids etc. Thus, the machined gears exhibited better surface quality with a good microstructure. Hence, no further machining or special tooling is required. Another advantage was observed as much less wastage of the composite material.

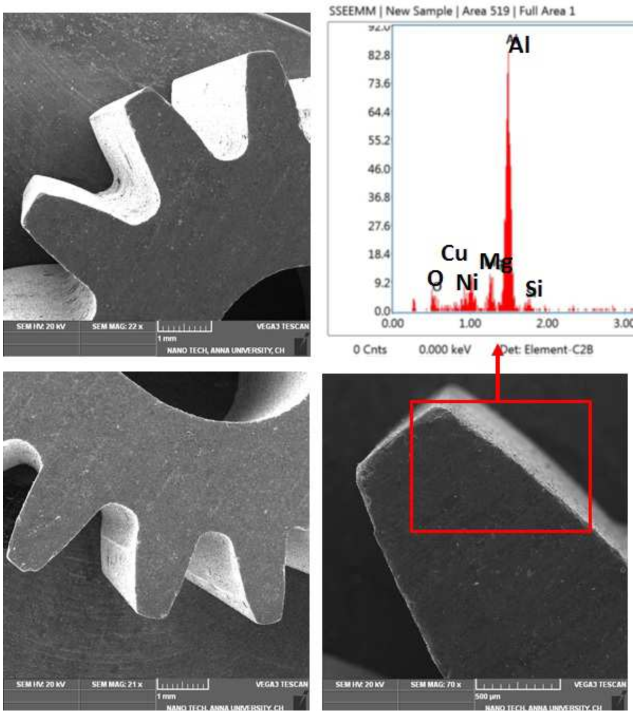


Fig. 9. SEM and EDAX of gear (Specimen 7)

## CONCLUSIONS

Taguchi's DOE was adopted to study the optimal machining parameters to manufacture 6 wt.% nickel-coated alumina-reinforced composite miniature gears. The consequences of the machining responses were analysed using Taguchi's analysis. The following are the conclusions obtained from the current study:

- The present investigation was modelled as a multi-objective optimization, which maximizes the MRR and minimizes the $R_a$.
- The largest value of GRG was obtained in experimental run 7, i.e. $T_{on}$ = 126 μs, $T_{off}$ = 45 μs and peak current = 165 A.
- From ANOVA, it was found that the pulse-on-time, pulse-off-time and peak current are the most significant parameters for the desired performance characteristics. Better quality miniature gears can be manufactured by utilizing suitable process parameters to attain high-strength gears.

The discussed Taguchi-based GRA methodology in the present investigation is the most appropriate to establish the best combination of process parameters to attain improved quality in the machining performance of the AA7075/Ni-coated $Al_2O_3$ composite.

## REFERENCES


[1] Kumar S.D., Ravichandran M., Synthesis, characterization and wire electric erosion behaviour of AA7178-10 wt.% $ZrB_2$ composite, Silicon 2018, 10(6), 2653-2662, DOI: 10.1007/s12633-018-9802-7

[2] Srinivasan N., Rajenthira Kumar D., Sridhar R., Niranjan G., Combined influence of size effect and temperature in micro scale deformation of 6063 aluminum gear, J. Braz. Soc. Mech. 2020), 42(6), 1-10, DOI: 10.1007/s40430-020-02414-2.

[3] Rai P., Barman A.G., Design optimization of spur gear using SA and RCGA, J. Braz. Soc. Mech. 2018 40(5), 1-8, DOI: 10.1007/s40430-018-1180-y.

[4] Jain N.K., Chaubey S.K., Review of Miniature Gear Manufacturing, Elsevier 2017, DOI: 10.1016/B978-0-12-803581-8.09159-1.

[5] Gupta K., Jain N.K., Laubscher R.F., Spark erosion machining of miniature gears: a critical review, Int. J. Adv. Manuf. Technol. 2015, 80(9), 1863-1877, DOI: 10.1007/s00170-015-7130-2.

[6] Praveen D.V., Raju D.R., Raju M.J., Optimization of machining parameters of wire-cut EDM on ceramic particles reinforced Al-metal matrix composites – A review, Mater. Today: Proc. 2020, 23, 495-498, DOI: 10.1016/j.matpr.2019.05.392.

[7] Chaubey S.K., Jain N.K. On productivity of WSEM process for manufacturing meso-sized helical and bevel gears, IOP Conf. Ser.: Mater. Sci. Eng. 2018, July, 389, 1, 012007, IOP Publishing, DOI: 10.1088/1757-899X/389/1/012007.

[8] Alhadeff L.L., Curtis D.T., Marshall M.B., Slatter T., The application of wire electrical discharge machining (WEDM) in the prototyping of miniature brass gears, Procedia CIRP2018 77, 642-645, DOI: 10.1016/j.procir.2018.08.187.

[9] Chaubey S.K., Jain N.K., Investigations on surface quality of WEDM-manufactured meso bevel and helical gears, Mater. Manuf. Process 2018, 33(14), 1568-1577, DOI: 10.1080/10426914.2017.1415440.

[10] Ali M.Y., Mustafizul Karim A.N., Adesta E.Y.T., Ismail A.F., Idris M.N., Comparative study of conventional and micro WEDM based on machining of meso/micro sized spur gear, Int. J. Precis. Eng. 2010, 11(5), 779-784, DOI: 10.1007/s12541-010-0092-2.

[11] Praveen D.V., Raju D.R., Raju M.V.J., Nancharaiah T., A note on preparation of electroless nickel coating on alumina micro-particles as the forerunner to reinforce Al-MMCs, Recent Advances in Smart Manufacturing and Materials: Select Proceedings of ICEM 2020, 2021, 205, DOI: 10.1007/978-981-16-3033-0_19.

[12] Kumar D.S., Suman K.N.S., Kumar P.R., A study on electroless deposition of nickel on nano alumina powder under different sensitization conditions, Int. J. Adv. Manuf. Technol. 2016, 97, 59-68, DOI: 10.14257/ijast.2016.97.06.

[13] Praveen D.V., Raju D.R., Raju M.J., Influence of nickel coating of $Al_2O_3$ (P) reinforced AA-7075 metal matrix composites on hardness, impact strength and tensile properties, Mater.


 

Res. Express. 2019, 6(12), 126537, DOI: 10.1088/2053-1591/ab5594.

[14] Chandrasekar P., Nagaraju D., Improvement of bonding strength at the interfaces in scrap Al alloy composites using electroless Ni-P coated SiC, Silicon 2022, 14(6), 2941-2952, DOI: 10.1007/s12633-021-01078-4.

[15] Samal P., Surekha B., Vundavilli P.R., Experimental investigations on microstructure, mechanical behavior and tribological analysis of AA5154/SiC composites by stir casting, Silicon 2022, 14(7), 3317-3328, DOI: 10.1007/s12633-021-01115-2.

[16] Uğur A., Nas E., Gökkaya H., Investigation of the machinability of SiC reinforced MMC materials produced by molten metal stirring and conventional casting technique in die-sinking electrical discharge machine, Int. J. Mech. Sci. 2020, 186, 105875, DOI: 10.1016/j.ijmecsci.2020.105875.

[17] Vijay Praveen D., Ranga Raju D., Raju J., Assessment of optimal parameters of wire EDM on Ni-coated $Al_2O_3$p/AA7075 MMCs using PCA coupled GRA, Arab J. Sci. Eng. 2021, 46(8), 7953-7966, DOI: 10.1007/s13369-021-05579-7.

[18] Alam M.N., Siddiquee A.N., Khan Z.A., Khan N.Z., A comprehensive review on wire EDM performance evaluation, Proceedings of the Institution of Mechanical Engineers, Part E: Journal of Process Mechanical Engineering 2022, 236(4), 1724-1746, DOI: 10.1177/09544089221074843.

[19] Kumar N., Kumari S., Abhishek K., Nandi G., Ghosh N., Study on various parameters of WEDM using different optimization techniques: A review, Materials Today: Proceedings 2022, DOI: 10.1016/j.matpr.2022.04.596.

[20] Saha S.K., Choudhury S.K., Experimental investigation and empirical modeling of the dry electric discharge machining process, Int. J. Mach. Tools Manuf. 2009, 49(3-4), 297-308, DOI: 10.1016/j.ijmachtools.2008.10.012.

[21] Bellubbi S., Mallick B., Multi response optimization of ECDM process parameters for machining of micro channel in silica glass using taguchi-GRA technique, Silicon 2022, 14(8), 4249-4263, DOI: 10.1007/s12633-021-01167-4.

[22] Sonawane G.D., Sargade V.G., Evaluation and multi-objective optimization of nose wear, surface roughness and cutting forces using grey relation analysis (GRA), J. Braz. Soc. Mech. 2019, 41(12), 1-13, DOI: 10.1007/s40430-019-2057-4.

[23] Tosun N., Cogun C., Tosun G., A study on kerf and material removal rate in wire electrical discharge machining based on Taguchi method, J. Mater. Process. Technol. 2004, 152(3), 316-322, DOI: 10.1016/j.jmatprotec.2004.04.373.

[24] Kumar P., Meenu M., Kumar V., Optimization of process parameters for WEDM of Inconel 825 using grey relational analysis, Decis. Sci. Lett. 2018, 7(4), 405-416.

[25] Gupta K., Jain N.K., Deviations in geometry of miniature gears fabricated by wire electrical discharge machining, ASME International Mechanical Engineering Congress and Exposition (Vol. 56390, p. V010T11A047). American Society of Mechanical Engineers 2013, DOI: 10.1115/IMECE2013-66560.

[26] Shahbazi Dastjerdi M., Mokhtarian A., Saraeian P., The effect of alumina powder in dielectric on electrical discharge machining parameters of aluminum composite A413-$Al_2O_3$ by the Taguchi method, the signal-to-noise analysis and the total normalized quality loss, Int. J. Mech. Eng. 2020, 15, 1-11, DOI: 10.1186/s40712-020-00117-z.

 